Design of anti-icing surfaces: smooth, textured or slippery?

Michael J. Kreder[1], Jack Alvarenga[2], Philseok Kim[2] and Joanna Aizenberg[1−4]

Abstract | Passive anti-icing surfaces, or icephobic surfaces, are an area of great interest because of their significant economic, energy and safety implications in the prevention and easy removal of ice in many facets of society. The complex nature of icephobicity, which requires performance in a broad range of icing scenarios, creates many challenges when designing ice-repellent surfaces. Although superhydrophobic surfaces incorporating micro- or nanoscale roughness have been shown to prevent ice accumulation under certain conditions, the same roughness can be detrimental in other environments. Surfaces that present a smooth liquid interface can eliminate some of the drawbacks of textured superhydrophobic surfaces, but additional study is needed to fully realize their potential. As attention begins to shift towards alternative anti-icing strategies, it is important to consider and to understand the nature of ice repellency in all environments to identify the limitations of current solutions and to design new materials with robust icephobicity.

The ability to design materials that can withstand environmental challenges has been important for survival throughout human history. Critical issues, such as crop spoilage due to moisture contamination and hypothermia caused by the loss of body heat as a result of wet clothing, provided early motivation for the development of protective barriers that could effectively repel water in various forms, from condensed moisture to rain, snow and ice. Although some species have evolved features that allow them to resist the detrimental effects of water, such as the structure and hydrophobic properties of duck feathers, which can resist water penetration[1], humans have needed to develop broader technologies for repelling moisture in various situations. Typically, this has involved the selection of well-suited materials from nature, such as animal furs or natural fibres, which could then be further improved by incorporating natural oils and waxes to withstand harsh environments[2,3]. Such strategies provided the basis for water repellency until modern understanding of liquid–solid interactions allowed for the design of more advanced materials.

Pioneering work explained the nature of solid–liquid interactions, including wetting and non-wetting scenarios. In 1805, Thomas Young described the equilibrium behaviour of a droplet on an ideal surface[4]. Deviations in the contact angle of a droplet on a solid surface, which are critical to liquid adhesion and mobility, were first described as 'hysteresis' by the metallurgy community in the early 1900s[5], but the phenomenon was considered at least as far back as Gibbs's work on the thermodynamic properties of surfaces that included a discussion of "the frictional resistance to a displacement of the [contact] line" (REF. 6), and so-called contact angle hysteresis (CAH) continues to be investigated today[7–10]. Later developments led to further understanding of non-ideal surfaces through the Wenzel[11] and Cassie–Baxter[1,12] equations. For those readers who are unfamiliar with this foundational work, these theories are briefly described in BOX 1 and in detail by de Gennes and colleagues in REF. 13. Together, these theories established the surface characteristics that are required to yield highly effective water-repellent materials. A timeline of several major advances in repellency following Young's work is presented in FIG. 1.

Key materials advances in the development of water-repellent surfaces were the discovery of natural rubbers and the subsequent development of synthetic polymers in the 1900s[14]. This led to the production of important low-surface-energy polymers such as polydimethylsiloxane (PDMS; a common silicone rubber) and polytetrafluoroethylene (PTFE; commonly known as Teflon). Furthermore, by introducing porosity, PTFE could be made breathable and more water-repellent — a discovery that revolutionized the high-performance textile industry. These polymers can be applied as coatings on various materials to modify surface wettability. The development of an alternative method to create low-energy surfaces, which involves the self-assembly of molecular monolayers, allowed for the precise control of the surface chemistry and repellency of certain materials[15].

[1]John A. Paulson School of Engineering and Applied Sciences, Harvard University.
[2]Wyss Institute for Biologically Inspired Engineering, Harvard University.
[3]Department of Chemistry and Chemical Biology, Harvard University.
[4]Kavli Institute for Bionano Science and Technology, Harvard University, Cambridge, Massachusetts 02138, USA.
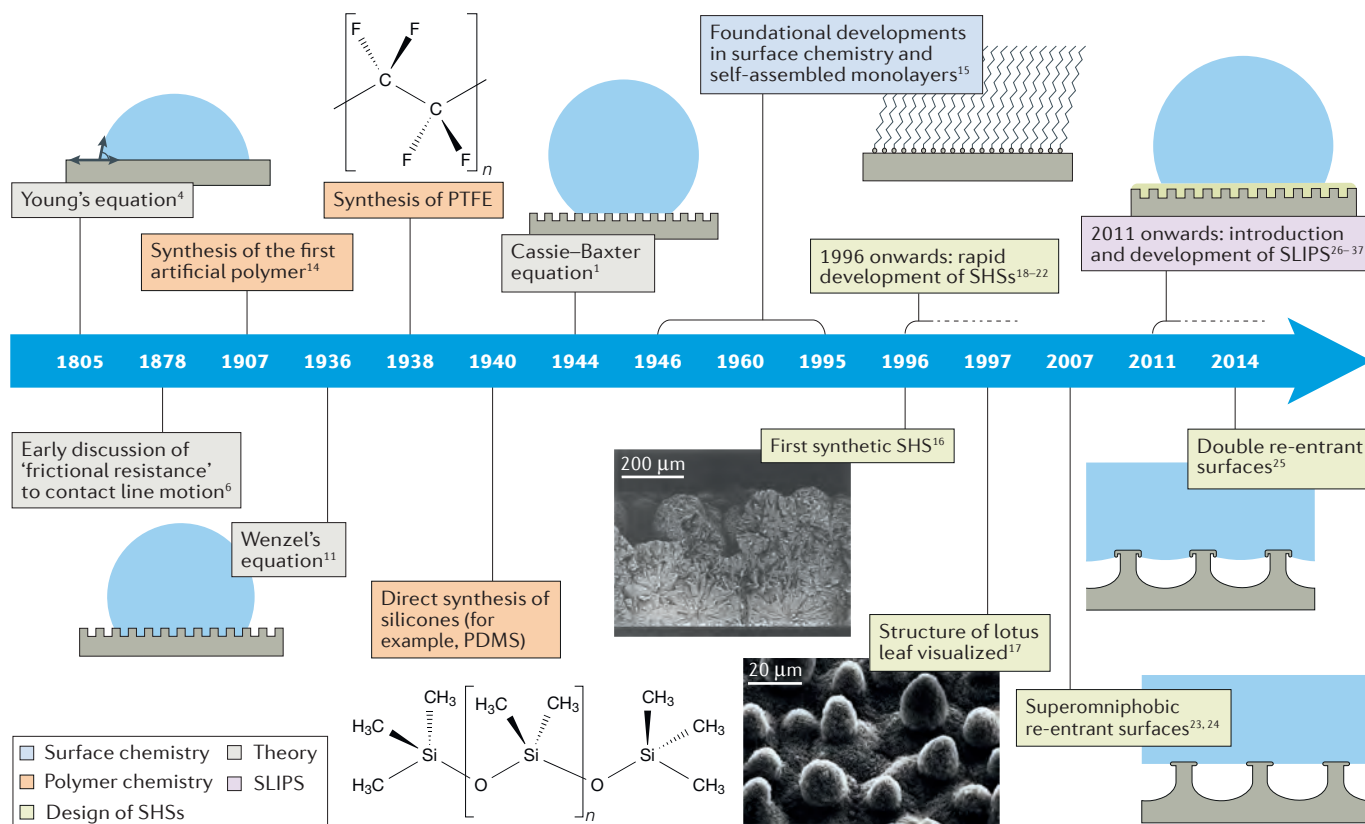
Correspondence to J.A.
jaiz@seas.harvard.edu

Figure 1 | Timeline of major advances in the area of liquid repellency. The timeline includes advances in theory, polymer and surface chemistry, as well as in the development of superhydrophobic surfaces (SHSs) and slippery liquid-infused porous surfaces (SLIPS). PDMS, polydimethylsiloxane; PTFE, polytetrafluoroethylene. The micrograph of the SHS is adapted with permission from REF. 16, American Chemical Society. The micrograph of the lotus leaf is adapted with permission from REF. 17, Springer.

In the late 1990s, advances in visualization and fabrication techniques sparked rapid developments in the area of water repellency. Specifically, the ability to visualize and replicate the structure of the lotus leaf enabled the production of synthetic superhydrophobic surfaces (SHSs) by combining micro- and nanoscale texture and hydrophobic surface chemistry, resulting in very high water contact angles (≥150°) and low CAH (≤5°)[16,17]. These discoveries led to a phase of extensive development, which saw SHSs produced from a wide array of materials and processes, with a concomitant improvement in performance and stability, and an increase in fundamental understanding[18–22]. The incorporation of re-entrant[23,24] and eventually double re-entrant[25] curvatures led to more robust repellency, resisting even low-surface-energy liquids that would completely wet typical nanostructured SHSs.

Although this complex surface structuring introduced enhanced repellency, the voids between surface features can serve as vulnerabilities under harsh environmental conditions. This problem was addressed by creating a new class of functional materials — slippery liquid-infused porous surfaces (SLIPS) — in which a textured solid is infiltrated with a physically and chemically confined immiscible lubricant to create a smooth liquid overlayer. The resulting surfaces are stable under high pressure, exhibit essentially no contact line pinning and are omniphobic[26–29]. Inspired by this approach, a variety of fabrication techniques for producing functional slippery surfaces have been reported, expanding the types of materials and potential applications this technology can advance[30–37].

Surfaces with low water wettability have been developed to possess many beneficial properties, such as fluid-flow drag reduction, increased heat transfer and improved self-cleaning ability[38–42]. In the challenging area of ice repellency, it has been shown that surfaces with low water wettability offer great promise as passive anti-icing — or icephobic — surfaces[40,41,43]; however, water repellency alone is not sufficient. Icephobic surfaces also require the ability to significantly suppress ice nucleation, to impede frost formation and to reduce ice adhesion forces. These challenges are the focus of this Review.

The nature of icing problems. Despite numerous advances in the development of repellent coatings, the problem of ice accretion remains significant[40,44,45]. Various critical structures, such as transmission lines and buildings, can be damaged by the excessive weight of accumulated ice and the stress caused by freeze–thaw cycles, and severe

personal injury can result from falling ice; such hazards are exacerbated by extreme conditions. Furthermore, in a marine environment, the preponderance of water leads to additional challenges on ships and off-shore oil rigs[45]. Transmission line and tower failures have led to notorious power outages, such as those caused by the 2008 ice storm in the northeastern United States, which left over 1 million people without power and an estimated cost for damages exceeding US$1 billion. The efficiency and output of renewable energy sources, including wind and solar, can also be severely affected by ice formation[43,46–48]. Ice accumulation on aircraft is responsible for several problems such as frequent delays, increased drag and numerous fatal crashes, while the use of salts and glycols in deicing fluids increases costs and leads to groundwater contamination[49,50]. Frost formation in a humid environment on cold solid surfaces, such as those commonly used in thermal management systems, can substantially reduce the heat transfer efficiency, with additional energy consumed during necessary defrosting cycles[40,41,51,52].

The diversity of icing problems presents many challenges. Icing conditions can only be controlled in certain environments. For example, heat exchangers may be designed to operate within narrow temperature and humidity ranges. However, in natural environments, ice accretion occurs over a wide range of temperatures, humidity levels and wind conditions owing to the many different forms of precipitation, including freezing rain, snow, in-cloud icing or fog icing, and frost formation[44,45]. Although it is typical for laboratory experiments to focus on a single aspect of icing, for many important applications icephobic materials require the ability to withstand a wide range of possible conditions. Current industry strategies for combatting icing problems primarily involve active heating, chemical deicing fluids and mechanical removal[44,49,50,53]. These processes can be inefficient, environmentally unfavourable, expensive and time consuming. Thus, it would be advantageous if surfaces could passively prevent ice formation and ease ice removal. In this Review, we critically examine various

---

Box 1 | Key concepts in liquid–solid interactions

The shape of a liquid droplet deposited on an ideal solid surface (smooth and chemically homogeneous) is dictated by an equilibrium of forces at the contact line formed by the three phases (solid, liquid and vapour). Young's equation relates the equilibrium contact angle (CA) of the droplet (θ) to the specific energies of the solid/liquid (γ_{sl}), solid/vapour (γ_{sv}), and liquid/vapour (γ_{lv}) interfaces.

Most surfaces feature some level of roughness, which can cause significant deviation from the ideal surfaces described by Young's equation. If a liquid droplet forms a continuously wetting interface along the topography of a solid surface, the apparent CA (θ^*) can be defined by the Wenzel equation, where r is the roughness factor, which is the ratio of the actual surface area to the projected surface area of the solid.

In the Cassie–Baxter state, liquid droplets do not fully conform to the topography of hydrophobic surfaces and rest on a composite interface composed of the peaks of the solid texture and trapped air pockets. This form of the Cassie–Baxter equation incorporates the relative contributions from the substrate and the air pockets on the CA of the liquid droplet, where ϕ_S is the solid area fraction of the substrate in contact with the liquid droplet. The equation can be generalized to apply to surfaces with heterogeneous surface energy.

Movement of the contact line can lead to variations in the CA as a result of surface protrusions, adhesion hysteresis, heterogeneity and thermodynamic considerations. The largest CA observed before the contact line advances is recognized as the advancing CA (θ_A). Conversely, the smallest CA observed before the contact line recedes represents the receding CA (θ_R). The difference between these CAs is defined as the contact angle hysteresis (CAH). Surfaces with low CAH allow for high-mobility droplets with low adhesion.
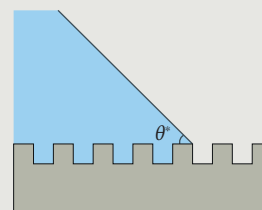
Young's equation

$$\cos(\theta) = \frac{\gamma_{sv} - \gamma_{sl}}{\gamma_{lv}}$$
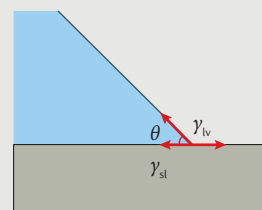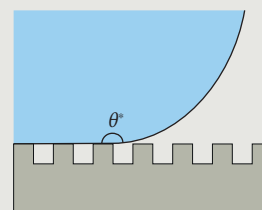

Wenzel's equation

$$\cos(\theta^*) = r\cos(\theta)$$
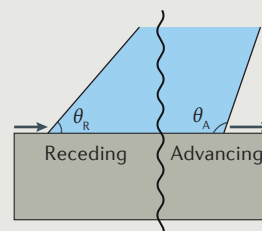

Cassie–Baxter equation
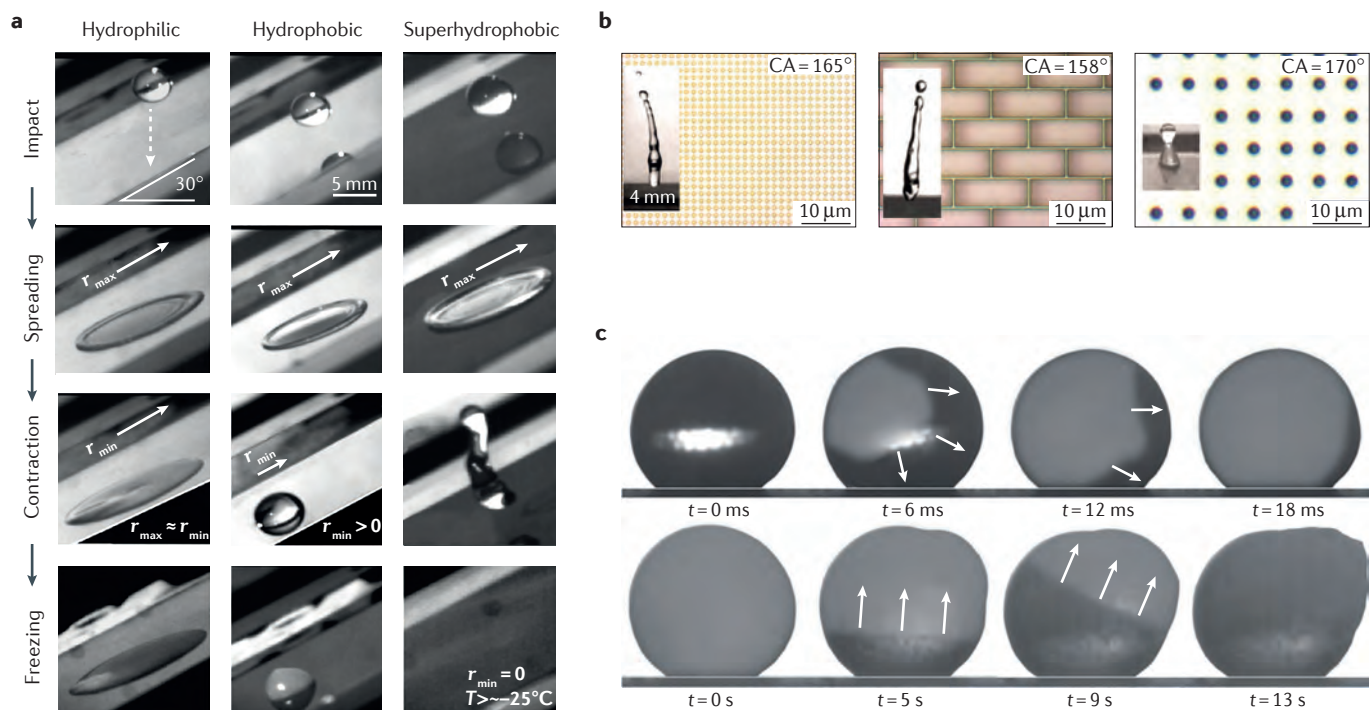
$$\cos(\theta^*) = -1 + \phi_s[\cos(\theta) + 1]$$

Contact angle hysteresis

$$\Delta\theta = \theta_A - \theta_R$$

Receding   Advancing

Figure 2 | Ice formation from impinging droplets. a | Droplets impacting a hydrophilic, a hydrophobic and a superhydrophobic surface. Only on the superhydrophobic surface are droplets able to fully retract and shed before freezing. **b** | Droplets are able to bounce on closely spaced posts (left panel) and a closed-cell architecture (middle panel), whereas they are pinned in the Wenzel state on posts with a larger spacing (right panel). **c** | Snapshots taken during the two phases of freezing for droplets exposed to unsaturated nitrogen flow. Partial solidification, initiated at the surface of the droplet, rapidly propagates through the entire volume (top panel). Following phase I, the remaining liquid freezes at a much slower rate that is controlled by heat transfer with the substrate and the environment (bottom panel). Arrows indicate the position and propagation direction of the freezing front during the two phases. CA, contact angle; r_{max}, maximum radius; r_{min}, minimum radius. Panels **a** and **b** adapted with permission from REF. 59, American Chemical Society. Panel **c** from REF. 84, Nature Publishing Group.

strategies for attaining icephobicity for the different scenarios in which ice may form on surfaces.

Ice formation from impinging droplets

Ice often accumulates when droplets of liquid water come into contact with surfaces that are at temperatures below the freezing point. This situation is commonly encountered in the form of freezing rain, and it affects aircraft, transmission lines and many other types of infrastructure[43,49]. SHSs, owing to their extraordinary water repellency, are viewed as excellent candidates for icephobicity in this area[40,54]; however, their performance is still largely limited by environmental constraints. In this scenario, ice formation can be prevented using two approaches: by minimizing the contact time to promote rapid shedding of droplets before ice can nucleate on the surface and by delaying heterogeneous nucleation through a combination of surface roughness, chemistry and topographical modifications.

Minimized contact time. It is well known that, under certain conditions, water droplets that impact a SHS will retract and bounce from the surface because of their extremely low CAH[55,56]. Taking advantage of this

phenomenon, SHSs can dynamically prevent ice formation, even if the surface is maintained at temperatures well below freezing[57–62], as shown in FIG. 2a. Mishchenko et al.[59] investigated impacting droplets with temperatures ranging from +60 to −5 °C onto substrates tilted by 30° and with surface temperatures ranging from +20 to −30 °C. Ice formation on the SHS was strongly dependent on the surface temperature, irrespective of the level of droplet undercooling. At surface temperatures above −25 °C, droplets were able to fully retract before freezing could occur on the SHS, whereas ice nucleated on smooth hydrophilic and hydrophobic surfaces[59]. Bahadur et al.[63] developed a detailed ice-formation model for a droplet impacting a structured SHS that incorporated the droplet contact time, heat transfer and heterogeneous nucleation theory. In their model, when a droplet strikes a supercooled surface, ice crystals nucleate on the tips of the posts, causing a decrease in the retraction force of the impacting droplet that eventually leads to incomplete retraction, pinning and complete freezing of the droplet; if the droplet contact time is less than the time required to induce pinning, then no ice forms. This transient model was found to be highly consistent with experimental results. More generally, the model demonstrated that the integration of multiple

dynamic processes, such as dynamic wetting, heat transfer and nucleation theory, is required to predict whether a surface resists ice formation[63].

Much of the work investigating droplet impact on SHSs has focused on increasing the stability of the Cassie state during droplet impingement in a freezing environment. Droplet bouncing occurs when the impacting liquid maintains enough energy to depart the surface following losses during spreading and retraction; however, if a droplet strikes the surface with sufficient kinetic energy, it may displace the air pockets of the SHS and become pinned in the Wenzel state[64–70]. Not only do droplets in this state have low mobility due to strong contact-line pinning, but their increased contact area with the underlying solid also improves heat transfer, leading to more opportunities for heterogeneous ice nucleation, even compared with topographically smooth hydrophobic surfaces[42].

The transition from the Cassie state to the Wenzel state is resisted by the Laplace pressure, which is the pressure difference across a curved interface caused by surface tension. The Laplace pressure can be increased by incorporating nanoscale topography[65–69], hierarchy[71] or using closed-cell structures[59,64], thereby resisting the transition into the Wenzel state, as shown in FIG. 2b. Improved icephobicity against impinging droplets has been demonstrated using denser features[57,59,72] or closed-cell structures[59]; however, increasing the solid fraction (ϕ_S) may instead lead to decreased superhydrophobic performance[68]. Ice nucleation could be further reduced by decreasing the contact time of bouncing droplets, which is possible by incorporating macroscopic texture on a SHS[73]; however, there is a practical limit to contact time on macroscopically smooth surfaces[73].

Another key consideration is the inability of SHSs to retain icephobicity under harsh environmental conditions. Lower temperatures increase the viscosity of supercooled droplets, thus increasing contact time and reducing the probability of bouncing[74]. In general, the bouncing-droplet effect is observed at low humidity levels. At surface temperatures below the dew point, the CAH of water droplets begins to increase owing to uniform nucleation across the surface topography of the microstructured SHS, which promotes non-bouncing Wenzel droplets[75–78]. In some cases, SHSs fail even in environments without bulk supersaturation because water droplets increase the humidity of their local environment[60]. Thus, in situations of high humidity or when supersaturation is likely to occur (typically when the surface is colder than the surrounding environment), the bouncing-droplet effect is an ineffective path towards icephobicity. For this reason, it is important to carefully consider environmental conditions related to real-world scenarios when testing these surfaces.

Nucleation reduction. Although the probability of nucleation can be reduced dynamically by promoting bouncing and rapid shedding of impinging droplets, it is also beneficial, particularly under static conditions, to delay heterogeneous nucleation through modification of surface topography and chemistry, which facilitates the potential removal of liquid water by other means. The ability of various surfaces to delay the freezing of a sessile droplet has been extensively studied to characterize the relationship between superhydrophobicity and heterogeneous ice nucleation, albeit with conflicting results. Many groups have found significantly delayed nucleation on microstructured SHSs[58,59,62,63], whereas other groups have found that nucleation is influenced more strongly by nanoscale roughness[57,75,79] or can be further influenced by hierarchical texture[80]. These discrepancies can be explained, at least in part, by the complexity of each system. There are multiple length scales to consider: the critical nucleus size required for the nucleation of ice (<10 nm)[75,79,80]; the nanoscopic surface roughness (<100 nm)[57,75,79–81]; the topography needed for superhydrophobicity (50 nm–10 µm)[58,59,62,63,80]; and the macroscopic droplet dimensions[58]. In addition, one must consider the effect of opportunistic nucleation sites on a sample[78], droplet impurities[58,82,83], surface chemistry[78,79,82,83] and environmental conditions such as wind, temperature and humidity[75,77,78,84]. All of these factors can work in concert or in competition, leading to results that are often difficult to decipher.

Classical nucleation theory has been well studied with regard to several phase-change scenarios[85] and is commonly applied to icephobic surfaces. Those who have reported nucleation delay on SHSs generally attribute this property to the insulating effect of the air pockets situated between the topographical features, to reduced solid–liquid contact area and to an increased free-energy barrier to heterogeneous nucleation[57–59,62,63,80]. Freezing delays were observed to be two orders of magnitude longer on microstructured SHSs compared with hydrophilic surfaces at surface temperatures of −20 °C; however, ice formed within seconds once the surface temperature was reduced to −25 °C (REF. 62). At low supercooling temperatures, it was suggested that homogeneous nucleation in the droplet and at the air/water interface dominates ice formation, limiting the effectiveness of surface-based approaches that prevent heterogeneous nucleation[62]. SHSs designed using 20-nm particles were found to have a lower ice nucleation probability than those designed with particles larger than 100 nm, possibly because the free-energy barrier for nucleation on the convex surface of 20-nm particles is higher than that for particles with greater radii of curvature[57]; however, the results can also be explained by the superior pressure stability of nanostructured surfaces.

By analysing surfaces with a range of chemistries and topographies, Jung *et al.*[79] found that hydrophilic surfaces with minimal roughness (1.4–6 nm) had the longest freezing-delay times, followed by hydrophobic surfaces with similar roughness, microstructured SHSs and finally hydrophilic microstructured surfaces. The lower rate of ice nucleation on hydrophilic surfaces with nanometre-scale surface roughness compared with equivalently smooth hydrophobic surfaces was also reported in experiments that eliminated the effect of droplet impurities by incorporating controlled evaporation, condensation and freezing processes[82,83]. Eberle *et al.*[80] found that although hydrophilic and hydrophobic surfaces with

ultrafine roughness exhibited similar nucleation temperatures (T_N), hydrophilic surfaces at temperatures slightly above T_N had a longer nucleation delay. The presence of a quasi-liquid layer with reduced entropy at the solid/water or solid/ice interface was seen as a key factor for reducing ice nucleation[79,80,82,83]. By adapting the classical theory of heterogeneous nucleation to account for a quasi-liquid layer, it was suggested that T_N could be lowered by minimizing the roughness length scale to below 10 nm (REFS 79–81). This hypothesis is supported by theoretical work proposing that the hydrogen bond network of water molecules is destabilized between hydrophobic surfaces when the inter-surface separation is on the order of 100 nm or less[86]. Eberle *et al.* further demonstrated that hierarchical SHSs that combine controlled nanoscale roughness with designed microtextures can increase the freezing delay at temperatures slightly above T_N by two orders of magnitude compared with hydrophobic nanostructured surfaces without microtextures[80]. At −21 °C, hierarchical SHSs delayed the freezing of a sessile drop by 25 hours (REF. 80).

In nature, organisms such as fish, insects and plants have evolved to produce antifreezing proteins, which suppress ice nucleation and growth in internal fluids. However, these proteins are generally not used by organisms or plants to prevent external ice accumulation[87–89]. There have been a number of recent attempts to incorporate antifreeze proteins into solid surfaces to develop icephobicity[90–92]. Although significant delays in ice nucleation have been observed using antifreeze proteins that were conjugated with polymer coatings[92] and directly immobilized on aluminium[90], one system, which incorporated antifreeze proteins on aluminium, instead showed increased ice nucleation owing to the favourable interaction of the surface proteins with the nucleating ice crystals[91]. More research is needed to determine the mechanism of ice nucleation in the presence of surface-bound antifreeze proteins and to develop practical strategies involving biomolecules for improved efficacy.

Although these controlled studies into ice nucleation are of great scientific interest, the ability to reduce the nucleation rate in practical scenarios is limited by environmental considerations. At temperatures below the dew point, many of the previously observed relationships governing ice nucleation behaviour on various surfaces could not be replicated[75,78]. The nucleation of ice on SHSs was systematically studied in an environmentally controlled wind tunnel, with tunable humidity and wind speed[84]. Under static conditions, the previously reported nucleation delay was observed; however, as shown in FIG. 2c, when there was a moderate flow of unsaturated gas, evaporative cooling of the water at the liquid/vapour interface induced homogeneous nucleation before heterogeneous nucleation at the solid surface[84]. A further consideration is surface contaminants, such as dust or salts, which serve as nucleation sites and lead to ice propagation across the surface[78,93]. These issues highlight some of the challenges facing icephobic materials in real-world environments. Even when heterogeneous nucleation is avoided on the surface itself, it is still possible for ice to accumulate.

Summary. Although the majority of work in this area has focused on the use of SHSs because of their unparalleled ability to shed liquid water through bouncing, limitations, particularly regarding humidity tolerance, have led some to explore alternatives. Sun *et al.*[76] were able to improve the performance of SHSs by combining an inner hydrophilic membrane suffused with a freezing-point depressant with an outer porous SHS, which separated the membrane from the environment. Under dry conditions, the surface behaved like an ordinary SHS, but when water penetrated the structure (under high pressure or humidity), the freezing-point depressant mixed with the water and prevented ice accumulation on the surface[76]. Techniques such as this may be necessary to provide icephobic surfaces that are robust enough to be used in a wide range of conditions, although the need for freezing-point depressants may preclude some applications. Another option is to use surfaces with stable lubricant interfaces[26,30]. Although droplet motion on SLIPS is typically slower than on SHSs due to viscous dissipation in the lubricant[94], the stability of the lubricant film under high droplet impact pressures[26,95] and their high humidity tolerance[26] may make SLIPS a viable alternative to SHSs in some scenarios. The advantages of such lubricated systems have predominantly been studied in frosting environments or in the context of ice adhesion, as we discuss in later sections.

Frost formation from atmospheric humidity

Although freezing experiments on impinging droplets are often carried out in low-humidity environments to eliminate the effects of condensation, performance in high-humidity environments is critical to many applications. For example, thermal management systems require that the condensate is promptly removed from the surface as it accumulates; otherwise, owing to reduced thermal conductance, water and frost will inhibit heat transfer[42,52]. Lubricant-infused surfaces, along with some specially designed SHSs, have shown promise in the rapid removal of condensation, thereby delaying frost formation under humid conditions.

Limitations of conventional superhydrophobic surfaces. When the temperature of a solid material falls below the dew point, water condensation occurs on the surface. On SHSs, condensed water droplets have been shown to nucleate and grow indiscriminately within hydrophobic microscale structures (FIG. 3a), as predicted by classical nucleation theory, which dictates that surfaces with spatially uniform interfacial energies will exhibit homogeneous nucleation energy barriers[81,96–100]. The larger surface area and confinement due to the microstructures serve to increase the rate of condensation on SHSs, which can result in the growing water droplets becoming trapped in the immobile Wenzel state[96–100]. Similar behaviour has been observed for the spatially non-preferential desublimation of frost on superhydrophobic microstructures[101].

This vulnerability to condensation can adversely affect the designed function of non-wetting surfaces, even in nature[102,103]. In one case, a water droplet placed
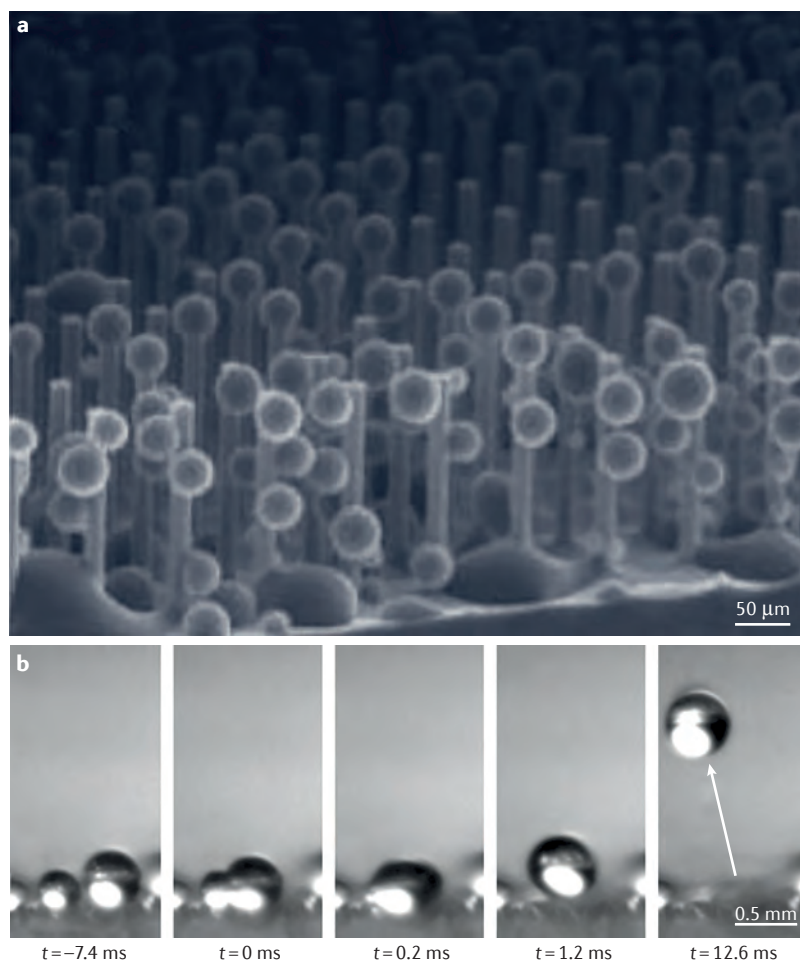
Figure 3 | Condensation on superhydrophobic surfaces. a | Environmental scanning electron microscopy image of the water vapour condensation behaviour on a microstructured superhydrophobic surface (SHS), whereby, owing to the chemical homogeneity of the surface, droplet nucleation occurs without apparent spatial preference. As these droplets grow and coalesce, Wenzel-type droplets are eventually formed. **b |** High-speed time-lapse images of autonomous out-of-plane droplet removal via dynamic coalescence observed on a hierarchical SHS with extremely low adhesion forces. $t = 0$ indicates the beginning of coalescence. Panel **a** adapted with permission from Varanasi, K. K., Hsu, M., Bhate, N., Yang, W. and Deng, T. Spatial control in the heterogeneous nucleation of water. *Appl. Phys. Lett.* **95**, 094101 (2009). Copyright 2009, AIP Publishing LLC. Panel **b** reprinted (figure) with permission from Boreyko, J. B. and Chen, C.-H. *Phys. Rev. Lett.* **103**, 184501 (2009). Copyright (2009) by the American Physical Society.

onto a surface patterned with fluorinated triangular microspikes was observed to be in the Cassie regime (contact angle = 164±3°; CAH = 5°)[104]. However, when the same surface was subjected to oversaturated vapour, water penetrated the cavities after progressive nucleation and coalescence events, resulting in a Wenzel wetting state. Although a relatively large contact angle of 141±3° was maintained, the CAH (100–105°) and droplet adhesion were significantly increased, thus preventing condensed droplets from being completely removed by external forces[104].

Surfaces incorporating dense nanoscale topography offer promising resistance against condensation-induced
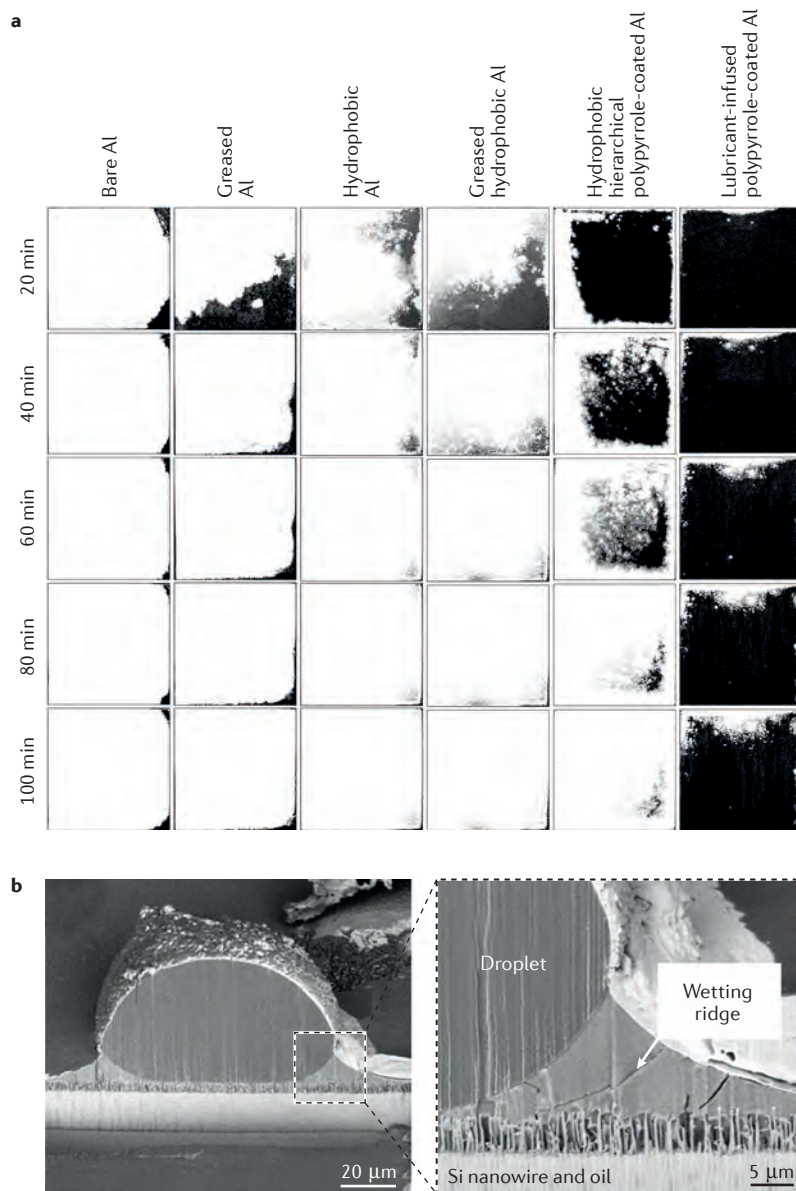
wetting and even display antifrosting behaviour[105–108]. Probably owing to the same mechanisms responsible for the delayed ice nucleation of sessile droplets on hydrophobic nanostructures[79,80], condensing droplets on nanostructured SHSs also experience longer freezing times[105–108]. These findings suggest that surfaces with minimized feature sizes that promote a Cassie state with low hysteresis would be more appropriate candidates in applications where liquid droplet mobility is desired during condensation.

Jumping droplet phenomenon. During conventional dropwise condensation on a flat hydrophobic surface, condensed water droplets typically exhibit high CAH, leading to large pinned droplets with diameters on the order of the capillary length of water (approximately 2.7 mm), which are only then able to be removed from the surface with the aid of gravity[109]. To remove smaller condensed microdroplets from the surface before freezing, new strategies have been developed. One such technique relies on nanostructured or hierarchical SHSs that, in certain scenarios, can promote spontaneous 'jumping-out-of-plane' removal of water microdroplets powered by the surface energy released on coalescence[110,111] (FIG. 3b). The spontaneous motion of droplets in such events is affected by various parameters, including the initial droplet volumes, viscous dissipation, surface feature sizes, structural hierarchy and work of adhesion[101,112–116].

This phenomenon of rapid removal of merged droplets is responsible for the extremely small average droplet size observed, ranging from approximately 6 to 30 μm (REFS 111,114). However, under conditions of high supersaturation, the emergent droplets transition from mobile jumping droplets to highly pinned Wenzel droplets, which completely flood the nanostructured cavities. This behaviour exposes the inherent limitations of this approach for high heat-flux applications[117]. Under high supersaturation conditions, the droplet nucleation density can increase to the point at which interactions between adjacent droplets occur on a similar length scale to the nanostructure spacing, causing the eventual formation of pinned liquid films[117].

The principle of self-propelled jumping droplets has been further applied to subcooling conditions under which droplets are able to repeatedly jump off the surface before heterogeneous ice nucleation can occur[118]. To circumvent limitations in supersaturation conditions, superhydrophobic nanostructured micropore arrays, with pitch spacing comparable to the diameter of coalescing microdroplets, have been introduced to maximize the liquid/air interfacial area beneath the coalescing microdroplets[119]. Although frost still forms, originating from physical or chemical defect sites, and eventually spreading over the entire surface via an interdrop frost wave, the growth of this frost front has been shown to be up to an order of magnitude slower on hierarchical SHSs than on a control hydrophobic surface[120]. Spatial control of heterogeneous droplet nucleation sites at the convex edges limits ice bridging and enhances the jumping droplet effect, which

dynamically minimizes the average droplet size and the overall surface coverage of the condensate[120]. Moreover, these nanostructured SHSs have also shown promise in active defrosting situations because the growth of frost can occur in a suspended Cassie state, enabling its dynamic removal upon partial melting at low tilt angles and preservation of the underlying surface[121].

Lubricant-infused surfaces. In the absence of air pockets, lubricant-infused surfaces can be expected to maintain high performance despite condensation. Under frosting conditions, a hierarchical SHS coating had over 90% of its surface covered in frost in 80 minutes, whereas its SLIPS counterpart experienced less than 20% coverage, mostly originating from edge defects and interdrop wave propagation[30,120], as shown in FIG. 4a. This delay can be attributed, in part, to the high mobility of droplets arising from low CAH, which allowed water droplets less than 600 μm in diameter to depart the surface under gravity before ice nucleation could occur[30]. An additional factor is the significantly increased supercooling ability (at least 3–4 °C freezing point depression compared with a SHS) of lubricant-infused surfaces. This property possibly arises because of a reduction in the number of potential nucleation sites, which was shown to be effective over 150 consecutive freeze–thaw cycles[122].

The repellency of these surfaces can be compromised by a loss of the lubricant overlayer, which can be driven by high shear, evaporation at high temperatures, gravity, or as a result of lubricant spreading onto other solid or liquid surfaces[94,123–126]. As with SHSs, detailed investigations have shown the importance of underlying surface roughness on performance. In the case of lubricant-infused structures, nanostructures are critically important for lubricant retention owing to the increased Laplace pressure, whereas the larger features of hierarchical structures more readily become exposed at the interface, leading to increased pinning[31,34,94,124,127]. Lubricant can spread over condensed droplets[128], as shown in FIG. 4b, which results in subsequent loss of the lubricant overlayer when droplets are shed. Careful selection of lubricant and favourable surface chemistry can prevent this effect and yield enhanced dropwise condensation behaviour[31]. Direct imaging of the microscale dynamics during condensation and frost formation on liquid-infused surfaces has provided insight into the interactions between the four phases (solid substrate, lubricant, water and air)[129].

Rykaczewski *et al.*[128] conducted a detailed study of frost formation on lubricant-infused structured surfaces using cryogenic scanning electron microscopy. This study highlighted the importance of nanoscale surface texture and optimized interfacial energies when designing lubricant-infused surfaces. Specifically, on surfaces with underlying microtexture, it was observed that the oil not only drained from the vicinity of a frozen droplet but also from underneath it, where it was permanently displaced by water, suggesting limitations in a prolonged droplet-shedding operation[128]. By contrast, increased capillary forces produced by nanotextured surfaces and proper surface functionalization are much more effective in retaining oil within the structures and limiting the subsequent penetration by water[31]. Although the anti-icing performance of these materials has been shown to rival that of state-of-the-art SHSs, careful design of the materials system is required to minimize lubricant migration and carry-over to achieve practical longevity.

Figure 4 | **Frost formation on different surfaces. a** | Time-lapse threshold images of frost formation (frost-covered areas shown in white) on various large-scale aluminium surfaces. After 100 min of freezing, ~99% of all control surfaces are covered with frost, except for the lubricant-infused polypyrrole coating, on which frost coverage was suppressed to only 20% of the area. **b** | Environmental scanning electron microscopy images of a frozen droplet on a lubricant-infused silicon nanowire surface, demonstrating the spreading and encapsulation of the droplet by the lubricant that can occur in unfavourable system configurations. Samples were cross-sectioned using a cryogenic focused ion beam. Panel **a** adapted with permission from REF. 30, American Chemical Society. Panel **b** adapted with permission from REF. 128, American Chemical Society.

Summary. Although superhydrophobicity alone is not sufficient to provide robust anti-frosting surfaces, when these surfaces are further engineered to induce jumping droplets, frost formation can be significantly delayed. However, the delicate nanoscale roughness required to promote jumping droplet behaviour is likely to result in surfaces prone to mechanical damage[130]. Alternatively, SLIPS can also shed small condensed droplets. These lubricant-infused surfaces are self-healing but require the overall lubricant level above the textured solid to be maintained, which may limit prolonged operation. The precise nature of condensation on SLIPS is still under investigation and, in some cases, is predicted to occur at the solid/lubricant interface[131]. Further understanding of this mechanism could influence the design of future frost-repellent materials.

Offering a potentially more robust approach to lubricated nanotextured surfaces, the incorporation of a lubricating oil into a bulk polymer or gel has recently been demonstrated as a high-performance repellent coating[132–137]. Aside from post-infusion of the polymer matrix with lubricant, it has been shown that the oil can be stored in discrete shell-less microdroplets within the polymer gel to provide a self-regulated liquid secretion directed towards the surface, which can also be made thermoresponsive for anti-icing applications[135,136]. If carefully designed and fabricated, these surfaces can exhibit most of the desirable traits of a functional anti-icing surface, including low surface energy, minimal surface roughness, a mobile oil overlayer and a longevity-enhancing lubricant reservoir. Although this approach offers a solution to lubricant loss by providing a surplus of oil, the underlying mechanism for lubricant depletion and the associated loss rate has not been addressed; for many applications, the additional weight gain and decreased heat transfer may counteract the potential benefits.

Adhesion of ice following freezing

Ice eventually forms on even the best icephobic surfaces under extreme conditions, making the easy removal of ice a critical but challenging requirement for icephobic materials. Fundamentally, the strong interaction of ice with most solids can be attributed to van der Waals forces[138] and electrostatic interactions[139], with the latter proposed as the dominant mechanism due to the interaction of electrical charge at the ice surface and induced charge on the solid substrate[139,140]. Surfaces that incorporate hydroxyl groups can also increase ice adhesion through hydrogen bonding[141]. Covalent chemical bonding directly associated with the ice surface can also be considered, but it is limited to very short distances (0.1–0.2 nm) and is only a factor for solids with specific chemical and crystal arrangements[139].

Although there are many different methods for measuring ice adhesion, the two most common techniques involve freezing a column of ice and shearing it from a surface using a force probe[142], or removing ice with the shear or tensile forces experienced during centrifugation[143]. It is worth noting that absolute values of ice adhesion (that is, the area-normalized force to remove ice) depend on the methods of measurement and ice formation[144]. To alleviate discrepancies between results, ice adhesion measurements can be normalized with respect to untreated control substrates, generating adhesion reduction factors, but there is no commonly accepted standard surface. Although aluminium is frequently used, variations in the surface quality, for example, due to surface finish or preparation, can still affect the results[144]. Thus, it is important to consider the specific methodology used for ice adhesion experiments and for researchers to incorporate adequate control surfaces to facilitate comparison. In FIG. 5, a broad overview is given of ice adhesion values reported in the literature[30,36,37,60,132,136,137,141,142,145–161], although this should be used only as a general guide owing to the aforementioned challenges. Ice adhesion below ~20 kPa is seen as the benchmark for surfaces that allow passive ice removal by factors such as wind or vibration; however, an ideal icephobic surface also requires high mechanical stiffness and durability[155,159,162]. Here, we focus on the relationship between water wettability and ice adhesion for smooth and structured surfaces before discussing recent strategies to reduce adhesion using lubricated surfaces.

Smooth and structured surfaces. Early attempts to minimize ice adhesion used predominantly smooth surfaces with low surface energy. Polymers such as PDMS[142] and PTFE[163] have been shown to minimize ice adhesion compared with higher-energy substrates, and there is a strong correlation between water wettability and ice adhesion[141,151,158]. In a comprehensive study that comprised a large number of smooth surface coatings, it was identified that the practical work of adhesion for water, $W_A = \gamma_{lv}(1 + \cos\theta_r)$, has the strongest correlation with ice adhesion[151], where γ_{lv} is the surface tension of the water/vapour interface and θ_r is the receding contact angle. Because it is not possible to attain a receding contact angle greater than ~120° on smooth surfaces using known chemistries[164], SHSs with nano- and microscale roughness were needed to achieve significantly reduced ice adhesion[61,148–150,165,166], with typical values in the range of 50–100 kPa (REF. 150). These low values of ice adhesion occur when SHSs maintain the Cassie state at supercooled temperatures[148] and feature low CAH[150], in addition to high contact angles. The reduced ice adhesion on SHSs is explained by the solid/ice interfacial energy, low solid/ice contact area and the presence of stress concentrators at the tops of microposts that may promote crack initiation and ice delamination[167].

Unfortunately, the durability of these surfaces continues to be a major concern. Repeated icing–shear- removal cycles and even less rigorous freeze–thaw cycles[60] have been shown to increase adhesion significantly as high-aspect-ratio surface features tend to be permanently damaged during ice removal[60,147,152,160]. Furthermore, these surfaces still suffer from poor humidity tolerance, as discussed in previous sections. When water trapped in the Wenzel state freezes, ice adhesion scales with the actual solid/ice contact area, resulting in ice adhesion that is higher than on chemically equivalent flat surfaces[101,168]. Other researchers have confirmed that ice
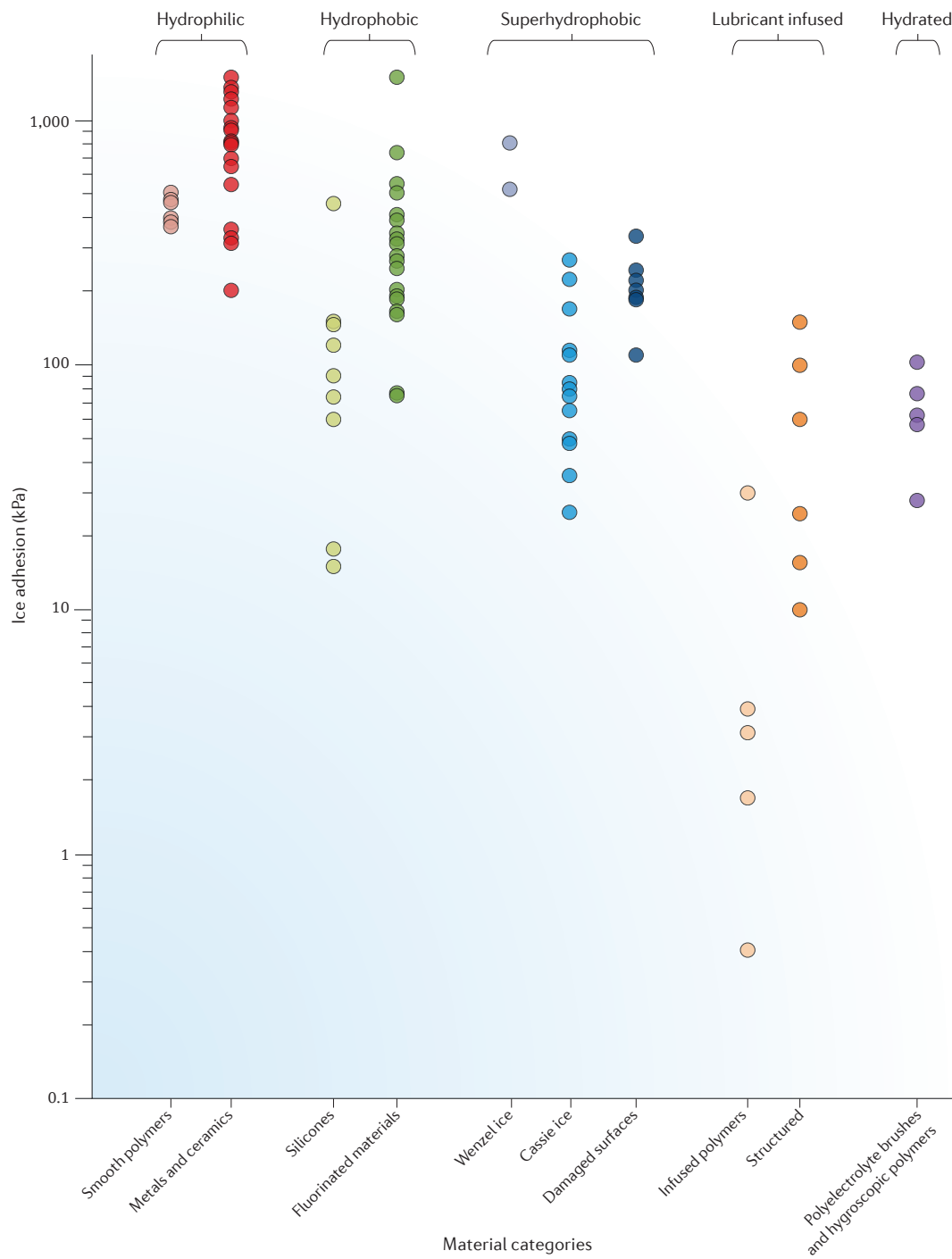
Figure 5 | **Ice adhesion values for different material categories.** Data is taken from the literature[30,36,37,60,132,136,137,141,142,145–161]. Ice adhesion has been shown to increase as the receding contact angle decreases on smooth surfaces[115].

formed in humid environments is much more difficult to remove[152,160] and may even form within microtextures in unsaturated environments owing to changes in local saturation caused by the latent heat of crystallization[169].

These limitations have renewed interest in the use of smooth surfaces to decrease ice adhesion[153,155,156]. Silicone-based coatings have been revisited as a potential material for decreasing ice adhesion, achieving very low

values[142,155,156], but testing viscoelastic polymer films adds a layer of complexity. Ice adhesion on PDMS surfaces has been shown to depend on both the film thickness and the strain rate during ice removal, compared with relatively constant values for stiff samples[155,156]. Furthermore, the low mechanical stiffness and durability of PDMS may make it unsuitable for some applications. Smooth fluorinated surfaces that are stiffer and more durable have

been developed in recent years[153,155]. In particular, smooth sol–gel coatings incorporating perfluorinated polyethers have been used to achieve an adhesion reduction factor of nearly 20 (approximate ice adhesion of 75 kPa)[155]. Maintaining low roughness was seen to be crucial to the performance of the coating[155], which was far superior to that of rough fluoropolymers[170].

Surfaces incorporating lubricant. Surfaces that incorporate a lubricating liquid have the potential to significantly reduce ice adhesion. Very low ice adhesion (~10–150 kPa) was observed on various structured, lubricant-infused surfaces[30,36,37,154,157]. These surfaces are thus at the upper threshold (that is, ~20 kPa) for self-removal of accreted ice by vibration or wind[155,159,162]. Subramanyam *et al.*[154] studied the dependence of ice adhesion on the lubricant level and found that ice adhesion increased significantly as excess lubricant above the posts was depleted; however, the extent to which ice adhesion increased was mitigated by spacing posts closely together. Although it may seem counter-intuitive that the surface with the highest solid fraction performed the best, the authors argued that ice adhesion was minimized by the high density of crack initiation sites at the edges of the posts[154]. Another effect that may contribute to decreased ice adhesion is the superior lubricant retention of closely spaced posts due to the increased Laplace pressure[127], which would allow closely spaced posts to maintain a smoother substrate/ice interface. Both factors should contribute to further reduce ice adhesion on lubricated surfaces incorporating nanostructures. As discussed with regard to frost formation, the longevity and durability of the lubricant-infused surfaces are significant challenges for their implementation as icephobic surfaces, and the strategies discussed for improvement in that context remain important.

Very low ice adhesion has been demonstrated using lubricant-infused polymer systems[132,136,137,142], and infused polymers can be expected to maintain low ice adhesion even once the lubricant is depleted owing to their generally low surface energy and smooth surfaces. The ice adhesion of PDMS has been shown to decrease when silicone oil is mixed with the uncured PDMS precursors[132,142]. Similar effects can be achieved by swelling the cured polymer network with compatible oils[134,137]. Using liquid paraffin as the infused oil in a PDMS network, Wang *et al.*[137] were able to achieve extraordinarily low ice adhesion of only 1.7 kPa at temperatures as low as −70 °C, and ice adhesion remained below 10 kPa after 35 icing–deicing cycles measured over the course of 100 days. However, measurements were spaced over the 100-day period, which masked the kinetic aspects of lubricant depletion and replenishment that still need to be studied and understood to characterize the performance of such systems in practical scenarios. Showcasing the importance of understanding lubricant dynamics, almost negligible ice adhesion could be obtained on a surface designed to release lubricant at low temperatures[136].

One of the more intriguing properties of ice is the presence of a thin liquid-like transition layer at the ice surface, which can make ice slippery and has been used to explain various phenomena, such as the ability of skates to slide easily on ice[171–175]. Although the existence of pressure- or friction-induced liquid films at the surface are popular explanations for low friction on ice, both theories are largely inadequate and have fallen out of favour compared with arguments that attribute interfacial disordering and entropic effects to the presence of a quasi-liquid layer at the ice surface[171–175]. This effect has been used to reduce ice adhesion on hydrated surfaces that promote the existence of an aqueous lubricant layer without the need for additional oils that become depleted over time[145,146,159,161]. Although hydrophilic surfaces generally possess high ice adhesion, these surfaces, which comprise hygroscopic polymer films[145,159,161] or polyelectrolyte brushes[146] that swell with water, are capable of suppressing ice nucleation through molecular confinement. There generally exists a transition temperature, ranging from −10 to −53 °C, below which the lubricating film is not present and ice adhesion increases drastically[145,146,159,161]. The transition point can be lowered by tuning the chemistry of the hygroscopic polymer[145,159,161] and maximizing the entropic effect of the counterion on the aqueous film[146]. The highest performing surface was able to maintain a low ice adhesion value of ~25 kPa at temperatures down to −53 °C, even after 30 icing–deicing cycles[159].

Summary. There are several promising options for reducing ice adhesion under active development, and lubricated systems in particular have demonstrated extraordinarily low ice adhesion in various studies; however, their longevity and ability to maintain performance in different environments are important considerations that require further study, in the cases of both infused polymers and structured surfaces. Another concern for these materials, including those that maintain aqueous lubricant layers, is their ability to withstand mechanical abrasion and damage. By crosslinking a hygroscopic polymer inside silicon micropores to protect the bulk of the polymer from abrasion, Chen *et al.*[161] made a surface that maintained low ice adhesion after 80 abrasion cycles; however, the durability of these polymer coatings on their own has not been reported. SHSs have been studied far more extensively than lubricated surfaces, and, to our knowledge, SHSs that demonstrate satisfactorily low ice adhesion along with mechanical durability and cycle tolerance have not yet been realized. Further efforts should focus on increasing durability, for example, by incorporating stronger materials or structures designed to maintain superhydrophobicity after sustaining damage[130,176,177]. Many natural structured materials show combinations of strength and toughness that have been difficult to replicate synthetically. It is possible that further understanding of the origin of these properties may inspire the development of new, tougher, structured surfaces that can yield more durable icephobicity[178]. Continued investigation into smooth surfaces may be worthwhile, as their simplicity and durability may make them the most industrially feasible avenue for many applications, particularly when lubrication is not possible.
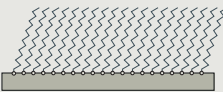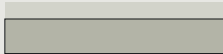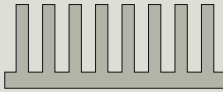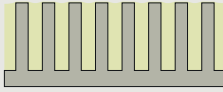
Perspective

Ice accumulation poses significant challenges in building infrastructure, marine applications, aerospace, refrigeration, power transmission, telecommunications and other industries. In this Review, we have focused on the various ways in which ice forms and passive prevention strategies that have been employed in each scenario. An ideal icephobic surface for many of these applications, however, should perform well in all possible situations. Although progress has been made, no single surface has shown the ability to rapidly shed impacting and condensing water droplets, suppress ice nucleation and reduce ice adhesion, all while operating in various environments with high durability and longevity. The strategies for developing icephobic materials, as discussed in this Review and shown in TABLE 1, include both dry and lubricated surfaces, spanning a range of chemical functionalities and length scales.

SHSs excel owing to their ability to shed water, but despite extensive research, issues of humidity tolerance and durability during ice removal persist. SHSs may be

Table 1 | **Comparison of primary strategies for achieving passive icephobicity**

Topology of surface	Type of surface	Properties	Refs
Dry			
Smooth	Self-assembled monolayer	• Environmentally tolerant • Limited surface compatibility • Lower performance than state of the art	141
	Bulk coatings	• Environmentally tolerant • Versatile and durable • Lower performance than state of the art	142,151,153,155, 156,163,170
Textured	Microstructured	• Rapid shedding of droplets prevents ice nucleation • Poor pressure and humidity tolerance • Poor durability	58,59,61–63,72, 74,79,101,158, 167,168
	Nanostructured	• Improved pressure stability • Improved humidity tolerance (jumping droplet effect) • Poor durability	57,60–62,72,75, 76,78–80,84,105, 108,118–121, 147–150,152,160, 165–167,169,170
Wet			
Smooth	Microstructured	• Low ice adhesion and droplet contact angle hysteresis • High humidity and pressure tolerance • Poor resistance to lubricant depletion	30,36,128,154
	Nanostructured	• Improved lubricant retention • Poor mechanical robustness	30,32,36,76, 122,128,157
	Infused polymer	• Increased lubricant content • Kinetics of lubricant depletion and replenishment unknown	132,136,137,142
	Hydrated	• Low ice adhesion without need for lubricant replenishment • Poor wetting properties	145,146,159,161

most effective when used in controlled environments, such as in heat exchangers, where the jumping droplet effect can delay frost formation and the surface can be maintained with limited exposure to the external environment. The ease of application and simplicity of smooth surfaces may make them attractive for use in harsher environments. Although the lack of nano- or microstructuring can make smooth surfaces more robust, roughness developed through erosion may still hinder repellency[155,170].

Hydrated surfaces with aqueous lubricating layers offer the advantage of simplicity and longevity because the lubricant can be replenished by atmospheric moisture; however, performance with respect to icephobic properties other than ice adhesion remains unreported. It can be expected that hydrophilicity will lead to poor resistance against impinging droplets and condensation. Further testing under various environmental conditions is needed to demonstrate the viability of hygroscopic polymers as widely applicable icephobic materials.

Surfaces incorporating hydrophobic lubricating layers continue to show extremely high promise, despite tempered expectations owing to current limitations on longevity. We anticipate that optimization of the topographical length scale, surface functionality and lubricant chemistry will be able to minimize these concerns. It is important not only to consider the empirical optimization of these parameters but also to gain a deeper understanding of the energetics and the interactions between components of this complex system. Infused polymers may offer improved longevity compared with structured surfaces owing to the presence of excess oil in the bulk polymer network. Furthermore, a degree of icephobicity should be maintained even on depletion of the lubricant owing to the remaining smooth, low-energy surface of the polymer. Future research should focus on durability, longevity and potential replenishment of these lubricant-infused surfaces rather than achieving maximum performance under ideal conditions.

Although passive ice-repellent materials continue to be improved, each has limitations in some aspects of icephobicity. By understanding the successes and failures of each technology, it may be possible to design surfaces that incorporate features from multiple strategies to further improve versatility. Ultimately, it may be necessary to use ice-repellent surfaces to augment, rather than completely eliminate, traditional anti-icing and deicing techniques. The work of Sun et al.[76], in which a SHS was used, stands out as a method for reducing the amount of deicing fluid used on airplanes. Such a technique might also be combined with biological or biomimetic antifreeze proteins to offer a more environmentally friendly solution. One can imagine similar strategies, such as surfaces with low wettability being used to decrease the amount of heating needed to remove ice, or lubricant-infused surfaces that release lubricant only under certain environmental conditions[136]. The integration of icephobic materials with current technologies has not seen extensive study, but it is an important consideration for the eventual application of these materials.

1. Cassie, A. B. D. & Baxter, S. Wettability of porous surfaces. *Trans. Faraday Soc.* **40**, 546–551 (1944).
2. Holman, H. P. & Jarrell, T. D. The effects of waterproofing materials and outdoor exposure upon the tensile strength of cotton yarn. *Ind. Eng. Chem.* **15**, 236–240 (1923).
3. McBurney, D. Coated fabrics in construction industry. *Ind. Eng. Chem.* **27**, 1400–1403 (1935).
4. Young, T. An essay on the cohesion of fluids. *Phil. Trans. R. Soc.* **95**, 65–87 (1805).
5. Rickard, T. A. & Ralston, O. C. *Flotation* (Mining and Scientific Press, 1917).
6. Gibbs, J. W. On the equilibrium of heterogeneous substances. *Trans. Connect. Acad. Arts Sci.* **3**, 343–524 (1878).
7. Eral, H. B., 't Mannetje, D. J. C. M. & Oh, J. M. Contact angle hysteresis: a review of fundamentals and applications. *Colloid Polym. Sci.* **291**, 247–260 (2013).
8. Krasovitski, B. & Marmur, A. Drops down the hill: theoretical study of limiting contact angles and the hysteresis range on a tilted plate. *Langmuir* **21**, 3881–3885 (2005).
9. Nosonovsky, M. Model for solid–liquid and solid–solid friction of rough surfaces with adhesion hysteresis. *J. Chem. Phys.* **126**, 224701 (2007).
10. Tadmor, R. Line energy and the relation between advancing, receding, and young contact angles. *Langmuir* **20**, 7659–7664 (2004).
11. Wenzel, R. N. Resistance of solid surfaces to wetting by water. *Ind. Eng. Chem.* **28**, 988–994 (1936).
12. Cassie, A. B. D. Contact angles. *Discuss. Faraday Soc.* **3**, 11–16 (1948).
13. de Gennes, P.-G., Brochard-Wyart, F. & Quéré, D. *Capillarity and Wetting Phenomena: Drops, Bubbles, Pearls, Waves* (Springer Science & Business Media, 2013).
14. Carraher, C. E. Jr *Introduction to Polymer Chemistry* (CRC, 2012).
15. Ulman, A. Formation and structure of self-assembled monolayers. *Chem. Rev.* **96**, 1533–1554 (1996).
16. Onda, T., Shibuichi, S., Satoh, N. & Tsujii, K. Super-water-repellent fractal surfaces. *Langmuir* **12**, 2125–2127 (1996).
17. Barthlott, W. & Neinhuis, C. Purity of the sacred lotus, or escape from contamination in biological surfaces. *Planta* **202**, 1–8 (1997).
18. Simpson, J. T., Hunter, S. R. & Aytug, T. Superhydrophobic materials and coatings: a review. *Rep. Prog. Phys.* **78**, 086501 (2015).
19. Liu, K. & Jiang, L. Metallic surfaces with special wettability. *Nanoscale* **3**, 825–838 (2011).
20. Si, Y. & Guo, Z. Superhydrophobic nanocoatings: from materials to fabrications and to applications. *Nanoscale* **7**, 5922–5946 (2015).
21. Quéré, D. Wetting and roughness. *Annu. Rev. Mater. Res.* **38**, 71–99 (2008).
22. Quéré, D. Non-sticking drops. *Rep. Prog. Phys.* **68**, 2495–2532 (2005).
23. Ahuja, A. et al. Nanonails: a simple geometrical approach to electrically tunable superlyophobic surfaces. *Langmuir* **24**, 9–14 (2008).
24. Tuteja, A. et al. Designing superoleophobic surfaces. *Science* **318**, 1618–1622 (2007).
25. Liu, T. L. & Kim, C.-J. C. Turning a surface superrepellent even to completely wetting liquids. *Science* **346**, 1096–1100 (2014).
26. Wong, T.-S. et al. Bioinspired self-repairing slippery surfaces with pressure-stable omniphobicity. *Nature* **477**, 443–447 (2011).
27. Lafuma, A. & Quéré, D. Slippery pre-suffused surfaces. *Europhys. Lett.* **96**, 56001 (2011).
28. Aizenberg, J., Aizenberg, M., Kang, S. H., Wong, T. S. & Kim, P. Slippery surfaces with high pressure stability, optical transparency, and self-healing characteristics. US patent 9-121-306 (2013).
29. Aizenberg, J., Aizenberg, M., Kang, S. H., Wong, T. S. & Kim, P. Slippery surfaces with high pressure stability, optical transparency, and self-healing characteristics. US patent 9-121-307 (2013).
30. Kim, P. et al. Liquid-infused nanostructured surfaces with extreme anti-ice and anti-frost performance. *ACS Nano* **6**, 6569–6577 (2012).
   This work establishes the potential of liquid-infused surfaces for icephobicity, demonstrating very low ice adhesion in addition to high performance in frosting environments that cause traditional SHSs to fail.
31. Anand, S., Paxson, A. T., Dhiman, R., Smith, J. D. & Varanasi, K. K. Enhanced condensation on lubricant-impregnated nanotextured surfaces. *ACS Nano* **6**, 10122–10129 (2012).
32. Manabe, K., Nishizawa, S., Kyung, K. & Shiratori, S. Optical phenomena and antifrosting property on biomimetics slippery fluid-infused antireflective films via layer-by-layer comparison with superhydrophobic and antireflective films. *ACS Appl. Mater. Interfaces* **6**, 13985–13993 (2014).
33. Ma, W., Higaki, Y., Otsuka, H. & Takahara, A. Perfluoropolyether-infused nano-texture: a versatile approach to omniphobic coatings with low hysteresis and high transparency. *Chem. Commun.* **49**, 597–599 (2013).
34. Sunny, S., Vogel, N., Howell, C., Vu, T. L. & Aizenberg, J. Lubricant-infused nanoparticulate coatings assembled by layer-by-layer deposition. *Adv. Funct. Mater.* **24**, 6658–6667 (2014).
35. Huang, X., Chrisman, J. D. & Zacharia, N. S. Omniphobic slippery coatings based on lubricant-infused porous polyelectrolyte multilayers. *ACS Macro Lett.* **2**, 826–829 (2013).
36. Liu, Q. et al. Durability of a lubricant-infused electrospray silicon rubber surface as an anti-icing coating. *Appl. Surf. Sci.* **346**, 68–76 (2015).
37. Vogel, N., Belisle, R. A., Hatton, B., Wong, T.-S. & Aizenberg, J. Transparency and damage tolerance of patternable omniphobic lubricated surfaces based on inverse colloidal monolayers. *Nat. Commun.* **4**, 2176 (2013).
38. Bhushan, B. Biomimetics inspired surfaces for drag reduction and oleophobicity/philicity. *Beilstein J. Nanotechnol.* **2**, 66–84 (2011).
39. Liu, K. & Jiang, L. Bio-inspired self-cleaning surfaces. *Annu. Rev. Mater. Res.* **42**, 231–263 (2012).
40. Lv, J., Song, Y., Jiang, L. & Wang, J. Bio-inspired strategies for anti-icing. *ACS Nano* **8**, 3152–3169 (2014).
41. Zhang, P. & Lv, F. Y. A review of the recent advances in superhydrophobic surfaces and the emerging energy-related applications. *Energy* **82**, 1068–1087 (2015).

REVIEWS

42. Attinger, D. *et al.* Surface engineering for phase change heat transfer: a review. *MRS Energy Sustain.* **1**, E4 (2014).

43. Carriveau, R., Edrisy, A. & Cadieux, P. Ice adhesion issues in renewable energy infrastructure. *J. Adhes. Sci. Technol.* **26**, 37–41 (2012).

44. Laforte, J. L., Allaire, M. A. & Laflamme, J. State-of-the-art on power line de-icing. *Atmos. Res.* **46**, 143–158 (1998).

45. Ryerson, C. C. *Assessment of superstructure ice protection as applied to offshore oil operations safety: problems, hazards, needs, and potential transfer technologies* Report No. ERDC/CRREL TR-08-14 (US Army Corps of Engineers, 2008).

46. Laakso, T. *et al. State-of-the-art of wind energy in cold climates* Report No. VTT-WORK-152 (VTT Technical Research Centre of Finland, 2010).

47. Cucchiella, F. & Dadamo, I. Estimation of the energetic and environmental impacts of a roof-mounted building-integrated photovoltaic systems. *Renew. Sustain. Energy Rev.* **16**, 5245–5259 (2012).

48. Jelle, B. P. The challenge of removing snow downfall on photovoltaic solar cell roofs in order to maximize solar energy efficiency — research opportunities for the future. *Energy Build.* **67**, 334–351 (2013).

49. Gent, R. W., Dart, N. P. & Cansdale, J. T. Aircraft icing. *Phil. Trans. R. Soc. A* **358**, 2873–2911 (2000).

50. Environmental Protection Agency. *Effluent limitation guidelines and new source performance standards for the airport deicing category* (EPA, 2012).

51. U.S. Department of Energy. *Energy savings potential and R&D opportunities for commercial refrigeration final report* (Navigant Consulting, 2009).

52. Machielsen, C. H. M. & Kerschbaumer, H. G. Influence of frost formation and defrosting on the performance of air coolers: standards and dimensionless coefficients for the system designer. *Int. J. Refrig.* **12**, 283–290 (1989).

53. Leary, W. M. *We freeze to please: a history of NASA's icing research tunnel and the quest for flight safety* Report No. NASA SP-2002-4226 (NASA, 2002).

54. Schutzius, T. M. *et al.* Physics of icing and rational design of surfaces with extraordinary icephobicity. *Langmuir* **31**, 4807–4821 (2015).

55. Richard, D., Clanet, C. & Quéré, D. Contact time of a bouncing drop. *Nature* **417**, 811 (2002).

56. Richard, D. & Quéré, D. Bouncing water drops. *Europhys. Lett.* **50**, 769–775 (2000).

57. Cao, L., Jones, A. K., Sikka, V. K., Wu, J. & Gao, D. Anti-icing superhydrophobic coatings. *Langmuir* **25**, 12444–12448 (2009).

58. Tourkine, P., Le Merrer, M. & Quéré, D. Delayed freezing on water repellent materials. *Langmuir* **25**, 7214–7216 (2009).

59. Mishchenko, L. *et al.* Design of ice-free nanostructured surfaces based on repulsion of impacting water droplets. *ACS Nano* **4**, 7699–7707 (2010).
This study features an experimental analysis and proposed mechanism for the dynamic icephobicity of SHSs, which can rapidly shed incoming droplets before they freeze even at temperatures as low as −25 to −30 °C.

60. Wang, Y., Xue, J., Wang, Q., Chen, Q. & Ding, J. Verification of icephobic/anti-icing properties of a superhydrophobic surface. *ACS Appl. Mater. Interfaces* **5**, 3370–3381 (2013).

61. Ruan, M. *et al.* Preparation and anti-icing behavior of superhydrophobic surfaces on aluminum alloy substrates. *Langmuir* **29**, 8482–8491 (2013).

62. Alizadeh, A. *et al.* Dynamics of ice nucleation on water repellent surfaces. *Langmuir* **28**, 3180–3186 (2012).

63. Bahadur, V. *et al.* Predictive model for ice formation on superhydrophobic surfaces. *Langmuir* **27**, 14143–14150 (2011).

64. Bahadur, V. & Garimella, S. V. Preventing the Cassie–Wenzel transition using surfaces with non-communicating roughness elements. *Langmuir* **25**, 4815–4820 (2009).

65. Bartolo, D. *et al.* Bouncing or sticky droplets: impalement transitions on superhydrophobic micropatterned surfaces. *Europhys. Lett.* **74**, 299–305 (2006).

66. Reyssat, M., Yeomans, J. M. & Quéré, D. Impalement of fakir drops. *Europhys. Lett.* **81**, 26006 (2008).

67. Deng, T. *et al.* Nonwetting of impinging droplets on textured surfaces. *Appl. Phys. Lett.* **94**, 18–20 (2009).

68. Extrand, C. W. Designing for optimum liquid repellency. *Langmuir* **22**, 1711–1714 (2006).

69. Liu, B. & Lange, F. F. Pressure induced transition between superhydrophobic states: configuration diagrams and effect of surface feature size. *J. Colloid Interface Sci.* **298**, 899–909 (2006).

70. Ishino, C., Okumura, K. & Quéré, D. Wetting transitions on rough surfaces. *Europhys. Lett.* **68**, 419–425 (2007).

71. Boreyko, J. B., Baker, C. H., Poley, C. R. & Chen, C.-H. Wetting and dewetting transitions on hierarchical superhydrophobic surfaces. *Langmuir* **27**, 7502–7509 (2011).

72. Sarshar, M. A., Swarctz, C., Hunter, S., Simpson, J. & Choi, C. H. Effects of contact angle hysteresis on ice adhesion and growth on superhydrophobic surfaces under dynamic flow conditions. *Colloid Polym. Sci.* **291**, 427–435 (2013).

73. Bird, J. C., Dhiman, R., Kwon, H. M. & Varanasi, K. K. Reducing the contact time of a bouncing drop. *Nature* **503**, 385–388 (2013).

74. Maitra, T. *et al.* Supercooled water drops impacting superhydrophobic textures. *Langmuir* **30**, 10855–10861 (2014).

75. Heydari, G., Thormann, E., Ja, M., Tyrode, E. & Claesson, P. M. Hydrophobic surfaces: topography effects on wetting by supercooled water and freezing delay. *J. Phys. Chem. C* **117**, 21752–21762 (2013).

76. Sun, X., Damle, V., Liu, S. & Rykaczewski, K. Bioinspired stimuli-responsive and antifreeze-secreting anti-icing coatings. *Adv. Mater. Interfaces* **2**, 1400479 (2015).

77. He, M., Li, H., Wang, J. & Song, Y. Superhydrophobic surface at low surface temperature. *Appl. Phys. Lett.* **98**, 2009–2012 (2011).

78. Yin, L. *et al. In situ* investigation of ice formation on surfaces with representative wettability. *Appl. Surf. Sci.* **256**, 6764–6769 (2010).

79. Jung, S. *et al.* Are superhydrophobic surfaces best for icephobicity? *Langmuir* **27**, 3059–3066 (2011).

80. Eberle, P., Tiwari, M. K., Maitra, T & Poulikakos, D. Rational nanostructuring of surfaces for extraordinary icephobicity. *Nanoscale* **6**, 4874–4881 (2014).

81. Fletcher, N. H. Size effect in heterogeneous nucleation. *J. Chem. Phys.* **29**, 572–576 (1958).

82. Li, K. *et al.* Investigating the effects of solid surfaces on ice nucleation. *Langmuir* **28**, 10749–10754 (2012).

83. Li, K. *et al.* Viscosity of interfacial water regulates ice nucleation. *Appl. Phys. Lett.* **104**, 10–14 (2014).

84. Jung, S., Tiwari, M. K., Doan, N. V. & Poulikakos, D. Mechanism of supercooled droplet freezing on surfaces. *Nat. Commun.* **3**, 615 (2012).
This study examines the mechanism of ice nucleation and growth in supercooled droplets deposited on various surfaces, particularly highlighting the effect of environmental factors such as humidity and airflow.

85. Kalikmanov, V. I. *Nucleation Theory* Vol. 860 (Springer, 2013).

86. Lum, K., Chandler, D. & Weeks, J. D. Hydrophobicity at small and large length scales. *J. Phys. Chem. B* **103**, 4570–4577 (1999).

87. Ewart, K. V., Lin, Q. & Hew, C. L. Structure, function and evolution of antifreeze proteins. *Cell. Mol. Life Sci.* **55**, 271–283 (1999).

88. Clark, M. S. & Worland, M. R. How insects survive the cold: molecular mechanisms—a review. *J. Comp. Physiol. B* **178**, 917–933 (2008).

89. Atıcı, Ö. & Nalbantoğlu, B. Antifreeze proteins in higher plants. *Phytochemistry* **64**, 1187–1196 (2003).

90. Gwak, Y. *et al.* Creating anti-icing surfaces via the direct immobilization of antifreeze proteins on aluminum. *Sci. Rep.* **5**, 12019 (2015).

91. Charpentier, T. V., Neville, A., Millner, P., Hewson, R. & Morina, A. An investigation of freezing of supercooled water on anti-freeze protein modified surfaces. *J. Bion. Eng.* **10**, 139–147 (2013).

92. Esser-Kahn, A. P., Trang, V. & Francis, M. B. Incorporation of antifreeze proteins into polymer coatings using site-selective bioconjugation. *J. Am. Chem. Soc.* **132**, 13264–13269 (2010).
Using antifreeze proteins found in Arctic fish and insects, a polymer–protein conjugate is demonstrated that can inhibit frost formation when applied as a thin film on glass substrates.

93. Hao, Q. *et al.* Mechanism of delayed frost growth on superhydrophobic surfaces with jumping condensates: more than interdrop freezing. *Langmuir* **30**, 15416–15422 (2014).

94. Smith, J. D. *et al.* Droplet mobility on lubricant-impregnated surfaces. *Soft Matter* **9**, 1772–1780 (2013).

95. Lee, C., Kim, H. & Nam, Y. Drop impact dynamics on oil-infused nanostructured surfaces. *Langmuir* **30**, 8400–8407 (2014).

96. Narhe, R. D. & Beysens, D. A. Growth dynamics of water drops on a square-pattern rough hydrophobic surface. *Langmuir* **23**, 6486–6489 (2007).

97. Narhe, R. D. & Beysens, D. A. Nucleation and growth on a superhydrophobic grooved surface. *Phys. Rev. Lett.* **93**, 076103 (2004).

98. Wier, K. A. & McCarthy, T. J. Condensation on ultrahydrophobic surfaces and its effect on droplet mobility: ultrahydrophobic surfaces are not always water repellant. *Langmuir* **22**, 2433–2436 (2006).

99. Narhe, R. D. & Beysens, D. A. Water condensation on a super-hydrophobic spike surface. *Europhys. Lett.* **75**, 98–104 (2007).

100. Varanasi, K. K., Hsu, M., Bhate, N., Yang, W. & Deng, T. Spatial control in the heterogeneous nucleation of water. *Appl. Phys. Lett.* **95**, 094101 (2009).

101. Varanasi, K. K., Deng, T., Smith, J. D., Hsu, M. & Bhate, N. Frost formation and ice adhesion on superhydrophobic surfaces. *Appl. Phys. Lett.* **97**, 234102 (2010).
This paper demonstrates the vulnerability of microstructured SHSs to frost formation and reveals the corresponding increase in ice adhesion that can occur when water is frozen in the Wenzel state.

102. Cheng, Y. T. & Rodak, D. E. Is the lotus leaf superhydrophobic? *Appl. Phys. Lett.* **86**, 1–3 (2005).

103. Mockenhaupt, B., Ensikat, H. J., Spaeth, M. & Barthlott, W. Superhydrophobicity of biological and technical surfaces under moisture condensation: stability in relation to surface structure. *Langmuir* **24**, 13591–13597 (2008).

104. Lafuma, A. & Quéré, D. Superhydrophobic states. *Nat. Mater.* **2**, 457–460 (2003).

105. Zhang, Q. *et al.* Condensation mode determines the freezing of condensed water on solid surfaces. *Soft Matter* **8**, 8285–8288 (2012).

106. Guo, P. *et al.* Icephobic/anti-icing properties of micro/nanostructured surfaces. *Adv. Mater.* **24**, 2642–2648 (2012).

107. Zhang, Y., Yu, X., Wu, H. & Wu, J. Facile fabrication of superhydrophobic nanostructures on aluminum foils with controlled-condensation and delayed-icing effects. *Appl. Surf. Sci.* **258**, 8253–8257 (2012).

108. Wen, M., Wang, L., Zhang, M., Jiang, L. & Zheng, Y. Antifogging and icing-delay properties of composite micro- and nanostructured surfaces. *ACS Appl. Mater. Interfaces* **6**, 3963–3968 (2014).

109. Beysens, D. Dew nucleation and growth. *Comptes Rendus Phys.* **7**, 1082–1100 (2006).

110. Chen, C. H. *et al.* Dropwise condensation on superhydrophobic surfaces with two-tier roughness. *Appl. Phys. Lett.* **90**, 23–25 (2007).

111. Boreyko, J. B. & Chen, C.-H. Self-propelled dropwise condensate on superhydrophobic surfaces. *Phys. Rev. Lett.* **103**, 184501 (2009).

112. Liu, T. Q., Sun, W., Sun, X. Y. & Ai, H. R. Mechanism study of condensed drops jumping on super-hydrophobic surfaces. *Colloids Surf. A* **414**, 366–374 (2012).

113. He, M. *et al.* Hierarchically structured porous aluminum surfaces for high-efficient removal of condensed water. *Soft Matter* **8**, 6680–6683 (2012).

114. Chen, X. *et al.* Nanograssed micropyramidal architectures for continuous dropwise condensation. *Adv. Funct. Mater.* **21**, 4617–4623 (2011).

115. Rykaczewski, K. *et al.* How nanorough is rough enough to make a surface superhydrophobic during water condensation? *Soft Matter* **8**, 8786–8794 (2012).

116. Feng, J., Qin, Z. & Yao, S. Factors affecting the spontaneous motion of condensate drops on superhydrophobic copper surfaces. *Langmuir* **28**, 6067–6075 (2012).

117. Miljkovic, N. *et al.* Jumping-droplet-enhanced condensation on scalable superhydrophobic nanostructured surfaces. *Nano Lett.* **13**, 179–187 (2013).

118. Boreyko, J. B. & Collier, C. P. Delayed frost growth on jumping-drop superhydrophobic surfaces. *ACS Nano* **7**, 1618–1627 (2013).

119. Zhang, Q. *et al.* Anti-icing surfaces based on enhanced self-propelled jumping of condensed water microdroplets. *Chem. Commun.* **49**, 4516–4518 (2013).

120. Chen, X. *et al.* Activating the microscale edge effect in a hierarchical surface for frosting suppression and defrosting promotion. *Sci. Rep.* **3**, 2515 (2013).

121. Boreyko, J. B. *et al.* Dynamic defrosting on nanostructured superhydrophobic surfaces. *Langmuir* **29**, 9516–9524 (2013).

122. Wilson, P. W. *et al.* Inhibition of ice nucleation by slippery liquid-infused porous surfaces (SLIPS). *Phys. Chem. Chem. Phys.* **15**, 581–585 (2013).

123. Wexler, J. S., Jacobi, I. & Stone, H. A. Shear-driven failure of liquid-infused surfaces. *Phys. Rev. Lett.* **114**, 168301 (2015).

124. Howell, C. *et al.* Stability of surface-immobilized lubricant interfaces under flow. *Chem. Mater.* **27**, 1792–1800 (2015).

125. Daniel, D., Mankin, M. N., Belisle, R. A., Wong, T. S. & Aizenberg, J. Lubricant-infused micro/nano-structured surfaces with tunable dynamic omniphobicity at high temperatures. *Appl. Phys. Lett.* **102**, 231603 (2013).

126. Wexler, J. S. *et al.* Robust liquid-infused surfaces through patterned wettability. *Soft Matter* **11**, 5023–5029 (2015).

127. Kim, P., Kreder, M. J., Alvarenga, J. & Aizenberg, J. Hierarchical or not? Effect of the length scale and hierarchy of the surface roughness on omniphobicity of lubricant-infused substrates. *Nano Lett.* **13**, 1793–1799 (2013).

128. Rykaczewski, K., Anand, S., Subramanyam, S. B. & Varanasi, K. K. Mechanism of frost formation on lubricant-impregnated surfaces. *Langmuir* **29**, 5230–5238 (2013).

129. Rykaczewski, K., Landin, T., Walker, M. L., Scott, J. H. J. & Varanasi, K. K. Direct imaging of complex nano- to microscale interfaces involving solid, liquid, and gas phases. *ACS Nano* **6**, 9326–9334 (2012).

130. Verho, T. *et al.* Mechanically durable superhydrophobic surfaces. *Adv. Mater.* **23**, 673–678 (2011).

131. Xiao, R., Miljkovic, N., Enright, R. & Wang, E. N. Immersion condensation on oil-infused heterogeneous surfaces for enhanced heat transfer. *Sci. Rep.* **3**, 1988 (2013).

132. Zhu, L. *et al.* Ice-phobic coatings based on silicon-oil-infused polydimethylsiloxane. *ACS Appl. Mater. Interfaces* **5**, 4053–4062 (2013).

133. Yao, X. *et al.* Fluorogel elastomers with tunable transparency, elasticity, shape-memory, and antifouling properties. *Angew. Chem. Int. Ed. Engl.* **53**, 4418–4422 (2014).

134. MacCallum, N. *et al.* Liquid-infused silicone as biofouling-free medical material. *ACS Biomater. Sci. Eng.* **1**, 43–51 (2015).

135. Cui, J., Daniel, D., Grinthal, A., Lin, K. & Aizenberg, J. Dynamic polymer systems with self-regulated secretion for the control of surface properties and material healing. *Nat. Mater.* **14**, 790–795 (2015).

136. Urata, C., Dunderdale, G. J., England, M. W. & Hozumi, A. Self-lubricating organogels (SLUGs) with exceptional synersis-induced anti-sticking properties against viscous emulsions and ices. *J. Mater. Chem. A* **3**, 12626–12630 (2015).

137. Wang, Y. *et al.* Organogel as durable anti-icing coatings. *Sci. China Mater.* **58**, 559–565 (2015).

138. Wilen, L. A., Wettlaufer, J. S., Elbaum, M. & Schick, M. Dispersion-force effects in interfacial premelting of ice. *Phys. Rev. B* **52**, 12426–12433 (1995).

139. Ryzhkin, I. A. & Petrenko, V. F. Physical mechanisms responsible for ice adhesion. *J. Phys. Chem.* **5647**, 6267–6270 (1997).

140. Hays, D. A. in *Fundamentals of Adhesion* (ed. Lee, L.-H.) 249–278 (Springer, 1991).

141. Petrenko, V. F. & Peng, S. Reduction of ice adhesion to metal by using self-assembling monolayers (SAMs). *Can. J. Phys.* **81**, 387–393 (2003).

142. Jellinek, H. H. G., Kachi, H., Kittaka, S., Lee, M. & Yokota, R. Ice releasing block-copolymer coatings. *Colloid Polym. Sci.* **256**, 544–551 (1978).

143. Laforte, C. & Beisswenger, A. *Icephobic material centrifuge adhesion test* in *IWAIS XI* (Anti-icing Materials International Laboratory, 2005).

144. Makkonen, L. Ice adhesion — theory, measurements and countermeasures. *J. Adhes. Sci. Technol.* **26**, 413–445 (2012).

145. Chen, J., Luo, Z., Fan, Q., Lv, J. & Wang, J. Anti-ice coating inspired by ice skating. *Small* **10**, 4693–4699 (2014).

146. Chernyy, S. *et al.* Superhydrophilic polyelectrolyte brush layers with imparted anti-icing properties: effect of counter ions. *ACS Appl. Mater. Interfaces* **6**, 6487–6496 (2014).

147. Farhadi, S., Farzaneh, M. & Kulinich, S. A. Anti-icing performance of superhydrophobic surfaces. *Appl. Surf. Sci.* **257**, 6264–6269 (2011).

148. Fu, Q. *et al.* Development of sol–gel icephobic coatings: effect of surface roughness and surface energy. *ACS Appl. Mater. Interfaces* **6**, 20685–20692 (2014).

149. Ge, L. *et al.* Anti-icing property of superhydrophobic octadecyltrichlorosilane film and its ice adhesion strength. *J. Nanomater.* **2013**, 1–5 (2013).

150. Kulinich, S. A. & Farzaneh, M. How wetting hysteresis influences ice adhesion strength on superhydrophobic surfaces. *Langmuir* **25**, 8854–8856 (2009).

151. Meuler, A. J. *et al.* Relationships between water wettability and ice adhesion. *ACS Appl. Mater. Interfaces* **2**, 3100–3110 (2010).
This comprehensive study establishes a link between the practical work of adhesion for liquid water and the ice adhesion on smooth surfaces with a broad range of chemistries.

152. Momen, G., Jafari, R. & Farzaneh, M. Ice repellency behaviour of superhydrophobic surfaces: effects of atmospheric icing conditions and surface roughness. *Appl. Surf. Sci.* **349**, 211–218 (2015).

153. Sojoudi, H., McKinley, G. H. & Gleason, K. K. Linker-free grafting of fluorinated polymeric cross-linked network bilayers for durable reduction of ice adhesion. *Mater. Horiz.* **2**, 91–99 (2015).

154. Subramanyam, S. B., Rykaczewski, K. & Varanasi, K. K. Ice adhesion on lubricant-impregnated textured surfaces. *Langmuir* **29**, 13414–13418 (2013).

155. Susoff, M., Siegmann, K., Pfaffenroth, C. & Hirayama, M. Evaluation of icephobic coatings — screening of different coatings and influence of roughness. *Appl. Surf. Sci.* **282**, 870–879 (2013).

156. Wang, C., Fuller, T., Zhang, W. & Wynne, K. J. Thickness dependence of ice removal stress for a polydimethylsiloxane nanocomposite: Sylgard 184. *Langmuir* **30**, 12819–12826 (2014).

157. Yin, X. *et al.* Integration of self-lubrication and near-infrared photothermogenesis for excellent anti-icing/deicing performance. *Adv. Funct. Mater.* **25**, 4237–4245 (2015).

158. Zou, M. *et al.* Effects of surface roughness and energy on ice adhesion strength. *Appl. Surf. Sci.* **257**, 3786–3792 (2011).

159. Dou, R. *et al.* Anti-icing coating with an aqueous lubricating layer. *ACS Appl. Mater. Interfaces* **6**, 6998–7003 (2014).

160. Kulinich, S. A., Farhadi, S., Nose, K. & Du, X. W. Superhydrophobic surfaces: are they really ice-repellent? *Langmuir* **27**, 25–29 (2011).

161. Chen, J. *et al.* Robust prototypical anti-icing coatings with a self-lubricating liquid water layer between ice and substrate. *ACS Appl. Mater. Interfaces* **5**, 4026–4030 (2013).

162. Beisswenger, A., Guy, F. & Laforte, C. *Advances in ice adherence and accumulation reduction testing at the anti-icing materials international laboratory (AMIL)* (Anti-icing Materials International Laboratory, 2010).

163. Saito, H., Takai, K. & Yamauchi, G. Water- and ice-repellent coatings. *Surf. Coatings Int.* **80**, 168–171 (1997).

164. Nishino, T., Meguro, M., Nakamae, K., Matsushita, M. & Ueda, Y. The lowest surface free energy based on $-CF_3$ alignment. *Langmuir* **15**, 4321–4323 (1999).

165. Kulinich, S. A. & Farzaneh, M. Ice adhesion on super-hydrophobic surfaces. *Appl. Surf. Sci.* **255**, 8153–8157 (2009).

166. Davis, A., Yeong, Y. H., Steele, A., Bayer, I. S. & Loth, E. Superhydrophobic nanocomposite surface topography and ice adhesion. *ACS Appl. Mater. Interfaces* **6**, 9272–9279 (2014).

167. Hejazi, V., Sobolev, K. & Nosonovsky, M. From superhydrophobicity to icephobicity: forces and interaction analysis. *Sci. Rep.* **3**, 2194 (2013).

168. Chen, J. *et al.* Superhydrophobic surfaces cannot reduce ice adhesion. *Appl. Phys. Lett.* **101**, 111603 (2012).

169. Boinovich, L. & Emelyanenko, A. M. Role of water vapor desublimation in the adhesion of an iced droplet to a superhydrophobic surface. *Langmuir* **30**, 12596–12601 (2014).

170. Yang, S. *et al.* Research on the icephobic properties of fluoropolymer-based materials. *Appl. Surf. Sci.* **257**, 4956–4962 (2011).

171. Jellinek, H. H. G. Liquid-like (transition) layer on ice. *J. Colloid Interface Sci.* **25**, 192–205 (1967).

172. Ryzhkin, I. & Petrenko, V. Violation of ice rules near the surface: a theory for the quasiliquid layer. *Phys. Rev. B* **65**, 012205 (2001).

173. Rosenberg, R. Why is ice slippery? *Phys. Today* **58**, 50–55 (2005).

174. Fletcher, N. H. Surface structure of water and ice. *Philos. Mag.* **7**, 255–269 (1962).

175. Fletcher, N. H. Surface structure of water and ice: II. A revised model. *Philos. Mag.* **18**, 1287–1300 (1968).

176. Jin, H., Tian, X., Ikkala, O. & Ras, R. H. A. Preservation of superhydrophobic and superoleophobic properties upon wear damage. *ACS Appl. Mater. Interfaces* **5**, 485–488 (2013).

177. Tesler, A. B. *et al.* Extremely durable biofouling-resistant metallic surfaces based on electrodeposited nanoporous tungstite films on steel. *Nat. Commun.* **6**, 8649 (2015).

178. Wegst, U. G. K., Bai, H., Saiz, E., Tomsia, A. P. & Ritchie, R. O. Bioinspired structural materials. *Nat. Mater.* **14**, 23–36 (2014).

Competing interests
J.A. and P.K. are founders of SLIPS Technologies.